DOI: 10.13009/EUCASS2019-100



# Modeling of the evolution of multiphase flow of combustion products in the chamber of propulsion system

*Valery A. Babuk, Nikita L. Budnyi, Dimitry I. Kuklin, Alexander A. Nizyaev*
*Baltic state technical university «VOENMEH»*
*1, First Krasnoarmeyskaya Str., St.-Petersburg, 190005, Russia*
*E-mail: Babuk@peterlink.ru*

## Abstract

A mathematical model of the evolution of multiphase combustion products flow for propulsion systems has been developed. It is based on the physical picture of the process formulated on the basis of the available experimental data. In accordance with this picture, agglomerates are the main source of evolution. A variety of physicochemical transformations of these particles and their relationship with gas phase and smoke oxide particles (SOP) properties are considered. The analysis of the phenomena that have the most significant effect on slag-formation has been carried out. It is shown that vapor-phase burning of agglomerate metal is one of the most significant phenomenon in this regard. It has been determined that properties of SOP most significantly affect two-phase losses of specific impulse. It is established that size of the SOP particles in the process of evolution increases significantly. The results of the study allow suggest that the evolution process has a significant impact on motor performance.

## Introduction

Solid propulsion systems are widely used in aerospace applications. One of the most commonly used types of propellants are aluminized propellants. Metal additions improve energetical properties of propellants. However, it causes a number of specific phenomena that significantly complicate intra-chamber processes. One of the main consequences of metal addition into propellants is a formation of condensed combustion products (CCP). The CCP properties determine intensity of the slag-formation in the chamber, specific impulse losses, stability of the motor operation and optical properties of combustion products. Thus, these properties significantly affect on efficiency of the propulsion system.
During the propellant combustion, condensed products (agglomerates and smoke oxide particles (SOP) [1-3]) are supplied into the gas phase. Agglomerates are products of enlargement of condensed substances in the surface layer of burning propellant. Their size ranges from tens to hundreds and even thousands of micrometers. SOP is a product of metal combustion near the surface of burning propellant. Their size ranges from tens to thousands of nanometers. Condensed and gaseous products form a multiphase flow, which is involved into evolution process in the combustion chamber. This process consists of interactions between phases and fractions of CCP, and it causes transformation of particle size and structure, chemical composition and temperature of the condensed and gas phases.
To date, several studies on the modeling of the evolution process have been performed [4–7]. The depth of study of the processes during evolution is different. It remains an open question about influence of various phenomena during evolution on motor performance.
The proposed work is devoted to analysis of the model of evolution developed by the authors, and identification of factors that have the most significant impact on motor performance.

### 1. Physical picture of the evolution process

The flow of combustion products is a multiphase medium involved in interconnected physicochemical and phase transformations. According to the results of the previous work [7-10], evolution process in the combustion chamber includes the following phenomena (Fig. 1):

- Motion of condensed products in the gas flow;
- Vapor-phase burning of Al agglomerates;
- SOPs transformation due to coagulation (Brownian, turbulent etc) and condensation of combustion products of aluminum;
- Formation and removal of gaseous products during chemical interaction between Al and $Al_2O_3$ within agglomerates;

DOI: 10.13009/EUCASS2019-100



- Structure transformation of agglomerates;
- SOP deposition on surfaces of agglomerates with possible chemical interaction with Al;

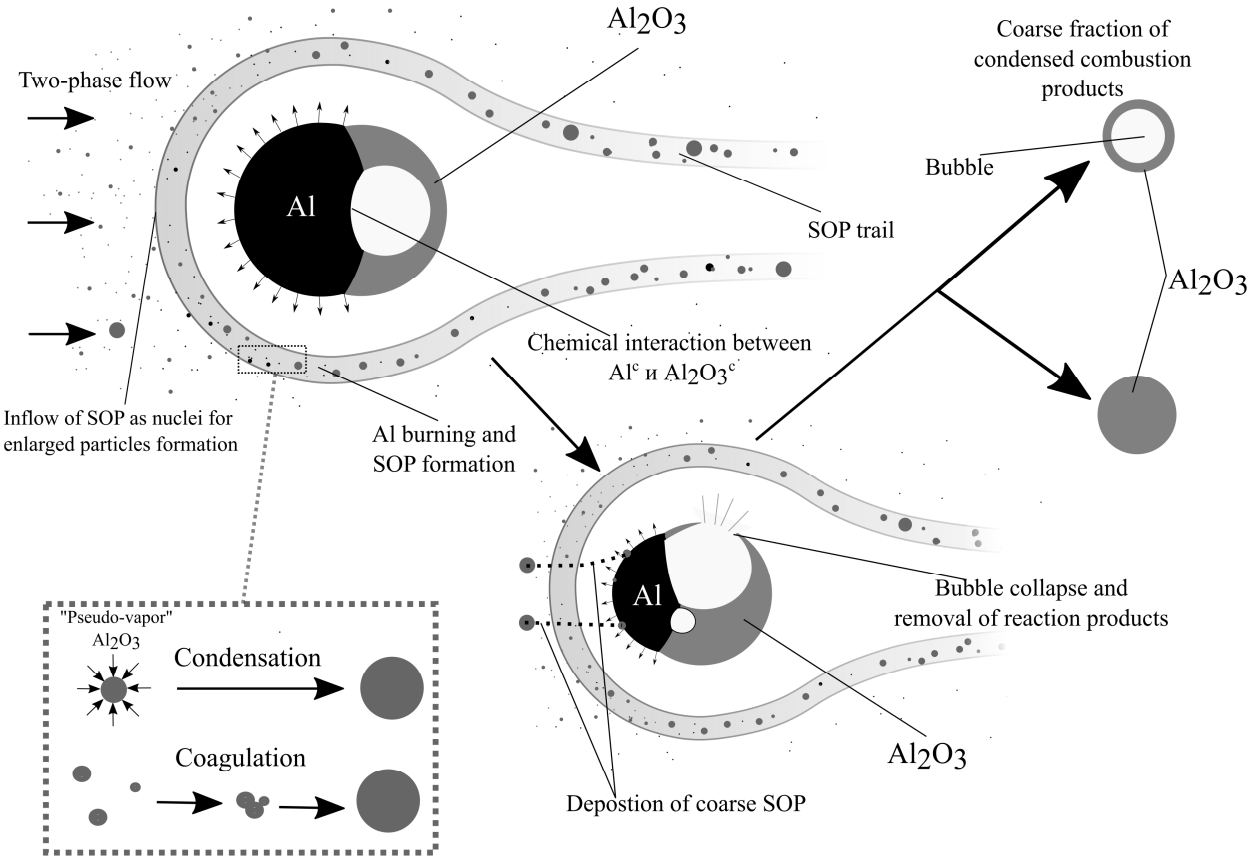


Figure 1: A diagram illustrating the evolution of combustion products

## 3. Mathematical model

Mathematical modeling is carried out through the synthesis of the models of individual phenomena during evolution process into the chamber. Let us consider these models.

### 3.1. Model of evolution of a single agglomerate

The description of the model is given in [11]. The model provides the following results:

- Rate of vapor-phase burning of metal;
- Kinetics of chemical interaction between condensed Al and $Al_2O_3$ with the formation of gaseous products;
- Structure of agglomerate;
- Intensity of deposition of SOP on agglomerate;
- Motion of agglomerate.

The input data of the model:
- Agglomerate properties (geometrical dimensions, chemical composition and structure, motion properties);
- Carrier gas phase properties (temperature, pressure, oxidation potential, SOP concentration and size, gas velocity field).

### 3.2. Model of SOP evolution

DOI: 10.13009/EUCASS2019-100



The simulation is based on concepts of SOP formation during agglomerate metal combustion [10, 12] and SOP involvement into the evolution process [13].
The simulation goal is to obtain mass and size of SOP along the curvilinear coordinate – $x_k$. SOP mass density function $f_m(d)$ of the ensemble is represented by discrete fractions. Every $i$-th fraction is described by its particle diameter $d$. It is assumed that SOP velocity corresponds to gas velocity.
Mathematical description of evolution of the SOP ensemble includes the system of ordinary differential equations for number density and particle mass for every fraction. At the elementary step $dx_k$, the SOP ensemble is divided into two parts – particles that interact and don't interact with agglomerates. Let us call these two types of particles as "interacting" and "noninteracting". Result of the interaction between SOP and agglomerates is enlargement of oxide particles due to condensation of aluminum suboxides on their surfaces and possible deposition of SOP particles on agglomerate surface. Size of "noninteracting" particles changes due to coagulation only.
The continuous approach is used for description of transformation of SOP size [14]: collision between particle of $i$-th fraction and coarser particle leads to decrease of number density of $i$-th fraction, collision between particle of $i$-th fraction and finer particle leads to increase of mass of $i$-th fraction particle.
Frequency of interactions between oxide particles form $i$-th fraction and agglomerates from $j$-th fraction can be calculated as:

$$\nu_{ij} = n_i \varepsilon^c_{ij} n_j^{aggl} \pi \left(R_j + r_i\right)^2 \Delta u_j \tag{3.1}$$

where $n$ – SOP number density, $n^{aggl}{}_j$ – number density of agglomerates from $j$-th fraction, $R$ – radius of agglomerate, $r$ – oxide particle radius, $\Delta u_j$ – velocity lag of agglomerates from $j$-th fraction, $\varepsilon^c{}_{ij}$ – coefficient of $i$-th fraction oxide particle entrapment into condensation zone of $j$-th fraction agglomerate.
Then, change of number density of "interacting" particles at $dx_k$:

$$dn_i^e = \frac{1}{u} \sum_{j=1}^{N_{aggl}} \nu_{ij} dx_k \tag{3.2}$$

where $u$ – gas and SOP velocity , $N_{aggl}$ – number of agglomerates fractions. Upper index «$e$» denotes the "interacting" particles. Upper index «0» denotes the "noninteracting" particles.
Dispersity transformation of "interacting" and "noninteracting" particles along $dx_k$ is described using the system of ODEs. For "noninteracting" particles the size transformation is described as follows:

$$\frac{dm_i^0}{dx_k} = \frac{1}{u} \sum_{j=1}^{i} n_j K_{ij}^{\Sigma} m_j \tag{3.3}$$

$$\frac{dn_i^0}{dx_k} = \frac{1}{u} \left(-n_i \sum_{j=1}^{i} n_j K_{ij}^{\Sigma} + w_i^0\right) \tag{3.4}$$

where $m$ – mass of the particle, $K^{\Sigma}_{ij}$ – total coagulation coefficient between particles of $i$-th and $j$-th fractions, $w^0{}_i$ – change of number density of $i$-th fraction due to transition of enlarged particles from finer fractions to $i$-th fraction and enlarged particles of $i$-th fraction to coarser fractions.
Size transformation of "interacting" particles is described in the same manner but considering additional mass sources and sinks related to interaction with agglomerates:

$$\frac{dm_i^e}{dx_k} = \frac{1}{u} \left(\sum_{j=1}^{i} n_j K_{ij}^{\Sigma} m_j + S_i I_{\Omega}\right) \tag{3.5}$$

$$\frac{dn_i^e}{dx_k} = \frac{1}{u} \left(-n_i \sum_{j=1}^{i} n_j K_{ij}^{\Sigma} + w_i^e - \sum_{j=1}^{N_{aggl}} \frac{\varepsilon^d_{ij}}{\varepsilon^c_{ij}} \nu_{ij}\right) \tag{3.6}$$

где $\varepsilon^d{}_{ij}$ –coefficient of deposition of the $i$-th fraction oxide particle on the j-th fraction agglomerate, $S_i$ – surface area of the $i$-th fraction particle, $I_{\Omega}$ - mass of attached suboxide vapor per unit area per unit of time, $w^e{}_i$ – similar to $w^0{}_i$ for "interacting particles".
Total change of number density in $i$-th fraction is:

DOI: 10.13009/EUCASS2019-100



$$\frac{dn_i}{dx_k} = \frac{dn_i^e}{dx_k} + \frac{dn_i^0}{dx_k} \tag{3.7}$$

The following algorithm is used: at the elementary step $dx_k$ number density of "interacting" particles can be calculated using (3.2); then one can calculate the derivatives (3.3, 3.5). It allows to integrate (3.4, 3.6) and calculate total change of umber density using (3.7). The algorithm is repeated for the next elementary steps.
Brownian and turbulent coagulation are considered. One can use the following relation:

$$K_{ij}^{\Sigma} = K_{ij}^{B} + K_{ij}^{TP} \tag{3.8}$$

Where the upper indexes denote respectively: «*B*» - Brownian coagulation, «*TP*» - turbulent coagulation.
Brownian coagulation coefficient can be calculated using the classical relation [18]:

$$K_{ij}^{B} = \frac{2}{3}\frac{(d_i + d_j)^2}{d_i d_j}\frac{kT}{\mu} \tag{3.9}$$

where: $d_i$, $d_j$ – diameters of $i$-th and $j$-th fraction particles, $k$ – Boltzmann constant, $T$ – temperature, $\mu$ – dynamic viscosity coefficient.
Heterogeneous structure of the composite solid propellant surface can act as a generator of turbulent pulsations. Detailed description of turbulent phenomena is a complex problem. Considering the conceptions of turbulent coagulation, [14-17], the following relation was proposed for an estimation of the turbulent coagulation coefficient in (3.8):

$$K_{ij}^{TP} \approx C_1 (d_i + d_j)^2 \left[ C_2 \left| d_i^2 - d_j^2 \right| + C_3 \frac{1}{(d_i + d_j)} \right] \tag{3.10}$$

where: $C_1$, $C_2$, $C_3$ – matching coefficients.
The values of $C_1$, $C_2$, $C_3$ were estimated using the experimental data on SOP size transformation during evolution in protective tubes [7]: $C_1$=5·10$^{-8}$, $C_2$=0.1 (m·s)$^{-1}$, $C_3$=1 m$^2$/s.
At the nozzle entrance, due to high acceleration of the gas phase, the appearance of coagulation caused by a different inertia of SOPs of different fractions is possible. In this situation, the additional term $K^{Vel}_{ij}$ should appear on the right-hand side of (3.8). Velocity lag for different SOP fractions for $K^{Vel}_{ij}$ calculation are estimated in the same manner as it was in [5].

### 3.3. Gas motion model

The following assumptions are made for description of gas phase motion:

- Flow is steady and axisymmetric;
- Gas is incompressible.

The model includes continuity and motion equations (Navier-Stokes equations).
The system is used as follows.

$$u_r \frac{\partial u_r}{\partial r} + u_z \frac{\partial u_r}{\partial z} = -\frac{1}{\rho}\frac{\partial P}{\partial r} + \frac{\mu}{\rho}\left( \frac{1}{r}\frac{\partial}{\partial r}\left( r \frac{\partial u_r}{\partial r} \right) + \frac{\partial^2 u_r}{\partial z^2} - \frac{u_r}{r^2} \right), \tag{3.11}$$

$$u_r \frac{\partial u_z}{\partial r} + u_z \frac{\partial u_z}{\partial z} = F_z - \frac{1}{\rho}\frac{\partial P}{\partial z} + \frac{\mu}{\rho}\left( \frac{1}{r}\frac{\partial}{\partial r}\left( r \frac{\partial u_z}{\partial r} \right) + \frac{\partial^2 u_z}{\partial z^2} \right), \tag{3.12}$$

$$\frac{1}{r}\frac{\partial (r u_r)}{\partial r} + \frac{\partial u_z}{\partial z} = 0, \tag{3.13}$$

where: $r$, $z$ – radial and longitudinal coordinates, m; $u_r$, $u_z$ – radial and longitudinal velocity components, m/s; $\rho$ – density, kg/m$^3$; $\mu$ – dynamic viscosity coefficient, Pa·s; $P$ – pressure, Pa; $F_z$ – mass longitudinal force, N/kg.
Boundary conditions depend on shape of the propellant grain channel, propellant burning rate, pressure, geometry of the chamber and pre-nozzle volume. The boundary conditions on the axis of symmetry:

DOI: 10.13009/EUCASS2019-100



$$u_z = 0, \quad \frac{\partial P}{\partial r} = 0, \quad \frac{\partial u_r}{\partial r} = 0, \quad \frac{\partial u_z}{\partial r} = 0, \tag{3.14}$$

On the wall of the combustion chamber:

$$u_r = 0 \, , \, u_z = 0 \, , \tag{3.15}$$

On the surface of the burning propellant:

$$u_r \rho = -r_{b_r} \rho_p , \quad u_z \rho = -r_{b_z} \rho_p , \tag{3.16}$$

In the output section of the combustion chamber:

$$P = P_0 \, , \tag{3.17}$$

where: $\rho_p$ – propellant density, kg/m$^3$; $r_{b_r}$ , $r_{b_z}$ – components of the burning rate of the propellant, m/s; $P_0$ – pressure in the combustion chamber, Pa.
The system of equations (3.11) - (3.13) with boundary conditions (3.14) - (3.17) is solved using the software implemented finite-volume method.
The solution of the system provides the definition of $u_r(r, z)$, $u_z(r, z)$, $P(r, z)$.

### 3.4. Model of the formation of the composition and temperature of the gas phase

The model is based on equilibrium thermodynamics [19]. It provides a calculation of temperature and chemical composition of the gas phase in a section of the streamtube, depending on parameter $Z_m$. This parameter is a ratio of the mass of metal burned within this streamtube to the mass of the initial metal supplied from the surface of the burning propellant.

### 3.5. Principles of calculation

The calculation is carried out by discretization of the computational domain in the motor combustion chamber. The discretization is carried out by creating a computational grid associated with gas phase streamlines. The cell of the grid is a streamtube of gaseous products. Within each *k*-th cell, a curvilinear coordinate system is built, the axis of which ( $x_k$ ) corresponds to the gas phase streamline (Fig. 2). The beginning of such a coordinate system is the propellant surface. The surface of the grain is divided into a set of sections that form streamtubes. In turn, the agglomerates supplied from the surface of the propellant are divided into a set of fractions. The trajectories of each agglomerate of the *i*-th fraction and the *j*-th site are calculated taking in account its evolution.
Modeling of agglomerates evolution within each streamtube allows one to find the parameters of agglomerates and gas phase along the curvilinear coordinate (Fig. 2). Initially, the calculation is carried out for the given values of the parameters of the gas phase and the SOPs for the entire computational domain. Then, the evolution of SOP within each streamtube is calculated. The calculations are repeated using the information from the previous iteration until the specified accuracy of determining the desired parameters is achieved.

DOI: 10.13009/EUCASS2019-100



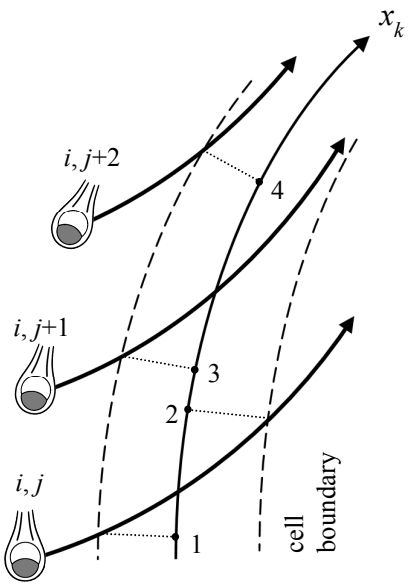


Figure 2: Cell of the computational domain and the trajectory of the agglomerates

## 4. Model analysis

Determination of the practical importance of CCP evolution effect on the motor performance is a significant concern. Apparently, we can talk about two processes associated with a presence of CCP, which have the most significant impact on a motor performance:
- Slag-formation in the combustion chamber;
- Two-phase losses of specific impulse.

Further analysis is aimed to estimation of the impact of evolution on these processes. The first process can be estimated by the intensity of CCP deposition on construction elements, the second – by the size of the CCP particles at the nozzle entrance.

For the analysis, it is necessary to set properties of the propellant, combustion conditions, properties of CCP supplied from the surface of the burning propellant, geometry of the computational domain.

The numerical analysis was performed for the propellant with experimentally obtained data on CCP properties [20] applied to conditions of the Castor 30 motor [21]. The calculations were performed for the initial and intermediate stages of the motor operation. The geometry of the computational domain is presented in Fig. 3

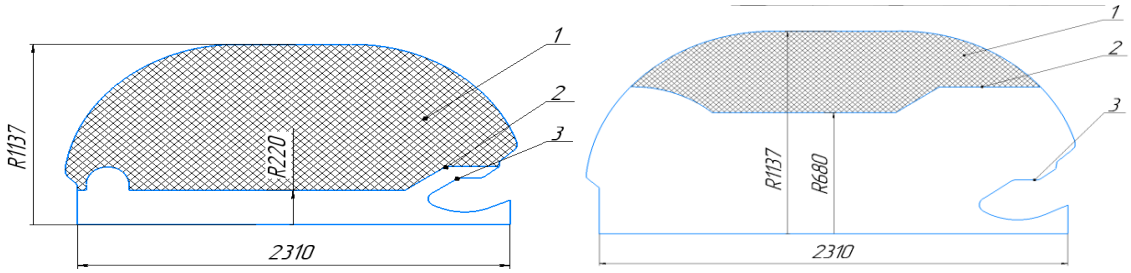


Figure 3: Geometrical dimensions of the combustion chamber at different points in time (1 – propellant grain, 2 – propellant burning surface, 3 – the wall affected by slag deposition).

### 4.1. Slag-formation

The considered process is mainly determined by agglomerate properties. The properties at the surface of the burning propellant are determined as follows:
– Diameter of agglomerate ($D_0$);

DOI: 10.13009/EUCASS2019-100



- mass fraction of oxide in agglomerates ($\eta_0$);
- the volume of the gas cavity in relation to the volume of the oxide drop ($\nu_{g_0}$);
- fraction of the original metal in the propellant used to form the agglomerates as a whole ($Z_m^a$).

According to the experimental result [20], these properties for selected propellant take values within the intervals given in table 1.

Table 1: Parameters of agglomerates at the propellant surface

| Parameter | Values |
|---|---|
| $D_0$ | 150 … 500 μm |
| $\eta_0$ | 0.3 … 0.95 |
| $\nu_{g_0}$ | 0 … $\nu_{g\max}$<br>$\nu_{g\max}$ - maximal possible value |
| $Z_m^a$ | 0.05…0.35 |

To estimate an impact of individual phenomena and total evolution impact on slag formation intensity, the calculation was carried out in several variants:

- Variant No 1. No agglomerates evolution simulation. Particle properties remains constant during motion.
- Variant No 2. No agglomerates evolution simulation. The agglomerates contain stationary gas cavities. Particle properties remains constant during motion.
- Variant No 3. Only the chemical interaction between an active metal of the agglomerate and its oxide is simulated.
- Variant No 4. Only vapor-phase burning of agglomerates is simulated.
- Variant No 5. All phenomenon during evolution are simulated.

It is advisable to compare results of particle deposition modeling with a “baseline” calculation variant. The variant No. 1 (without agglomerates evolution modeling) is selected as the “baseline”. This approach allows us to to make conclusions about contribution of various phenomena in slag-formation intensity. Results are presented as relative values $\kappa_i$ calculated using the following formula:

$$\kappa_i = \frac{M_{ag0} - M_{ag_i}}{M_{ag0}} \tag{4.1}$$

where: $\kappa_i$ – relative change in a mass flow of deposited agglomerates in the *i*-th variant of the calculation in relation to the first variant of the calculation, $M_{ag0}$ – mass flow of deposited agglomerates for 1 calculation variant, $M_{agi}$ – mass flow of deposited of agglomerates corresponding to the *i*-th variant of the calculation.

The calculation results of $\kappa_i$ for monodisperse agglomerate distribution are presented in tables 2-3 for the initial stage and in tables 3-4 for the intermediate stage ($Z_m^a$ = 0.344).

Table 2: Values of $\kappa_i$ at $\eta_0$ = 0.3

| Calculation variant / $D_0$, μm | 2 ($\nu_{g\max}$ =0.55) | 3 | 4 | 5 |
|---|---|---|---|---|
| 150 | 0 | 0.0188 | 0.1171 | 0.1359 |
| 300 | 0 | 0 | 0.0598 | 0.0610 |
| 500 | 0 | 0 | 0.022 | 0.0232 |

DOI: 10.13009/EUCASS2019-100



Table 3: Values of $\kappa_i$ at $\eta_0$ = 08.

| Calculation variant / $D_0$, μm | 2 ($\nu_{g\,max}$ =0.8) | 3 | 4 | 5 |
|---|---|---|---|---|
| 150 | 0.0507 | 0.0169 | 0.0689 | 0.0702 |
| 300 | 0.0306 | 0 | 0.0283 | 0.0283 |
| 500 | 0.016 | 0 | 0.0183 | 0.0183 |

Table 4: Values of $\kappa_i$ at $\eta_0$ = 0.3

| Calculation variant / $D_0$,μm | 2 ($\nu_{g\,max}$ =0.55) | 3 | 4 | 5 |
|---|---|---|---|---|
| 150 | 0.0591 | 0.1222 | 0.7389 | 0.7543 |
| 300 | 0.0201 | 0 | 0.3063 | 0.3082 |
| 500 | 0 | 0 | 0.1705 | 0.1696 |

Table 5: Values of $\kappa_i$ at $\eta_0$ = 0.8

| Calculation variant / $D_0$, μm | 2 ($\nu_{g\,max}$ =0.8) | 3 | 4 | 5 |
|---|---|---|---|---|
| 150 | 0.1384 | 0.0284 | 0.3027 | 0.3224 |
| 300 | 0.0801 | 0 | 0.1321 | 0.1399 |
| 500 | 0 | 0 | 0.0789 | 0.0789 |

The obvious consequence of the increase of a residence time of the combustion products in the motor chamber (initial - intermediate stages of work) is the increasing role of the evolution effect on a slag-formation. Maximal value of $\kappa_i$ for the initial stage is 0.1359, then for the intermediate stage it is 0.7543.

The most significant influence on slag formation is provided by a vapor-phase burning of the agglomerate metal (compared to other evolution phenomena). It leads to a decisive decrease in the size and mass of the agglomerates.

The effect of chemical interaction between condensed Al and $Al_2O_3$ appears only for relatively small agglomerates. This effect is associated with both certain oxide removal and formation of gas cavities.

The presence of gas cavities appears for agglomerates with relatively high oxide content.

Increasing of agglomerates size and oxide content, on the one hand, increases the intensity of slag-formation, and on the other, reduces the influence of the evolution process on slag-formation.

It should be noted that accuracy of vapor-phase burning of agglomerate metal modeling is determined by the validity of modeling of other phenomena during evolution (the formation of the structure of the agglomerates, the chemical interaction of condensed Al and $Al_2O_3$, etc.).

### 4.2. Two-phase loss of specific impulse

This type of losses depends on a size and mass of CCP at the nozzle entrance, and the nozzle geometry as well. In the framework of the analysis, the two-phase losses are determined by the size of the CCP.

The mass density size distributions of the coarse and the fine fractions of CCP at an intermediate stage of motor operation are given in Fig. 4-5. The calculations were performed for polydisperse distribution with the following initial data: $D_{43_0}$ = 257 μm, $\eta_0$= 0.4, $Z_m^a$ = 0.344 ($D_{43_0}$ -mass average diameter of agglomerates).

Due to the most significant realization of the evolution process for small agglomerates, their mass fraction decrease due to metal combustion, which leads to growth of the mean diameter of agglomerates. Let us note that the mass fraction of agglomerates is reduced by 50% during evolution. The parameter $Z_m^a$ at the nozzle entrance is 0.1817.

Thus, the bulk of the condensed products entering the nozzle are SOP, and properties of these particles have a decisive influence on two-phase losses. Enlargement of SOP occurs during evolution. The consequence of this process is a disappearance of the first mode of $f_m$ and the increasing SOPs mass average diameter – $d_{43}$. Figure 6

DOI: 10.13009/EUCASS2019-100



shows a dependence of $d_{43}$ along the curvilinear coordinate. Growth of SOPs is a result of condensation and coagulation. The effect of the deposition of SOP on agglomerates is negligible. Let us note the increasing role of inertial coagulation at the nozzle entrance.

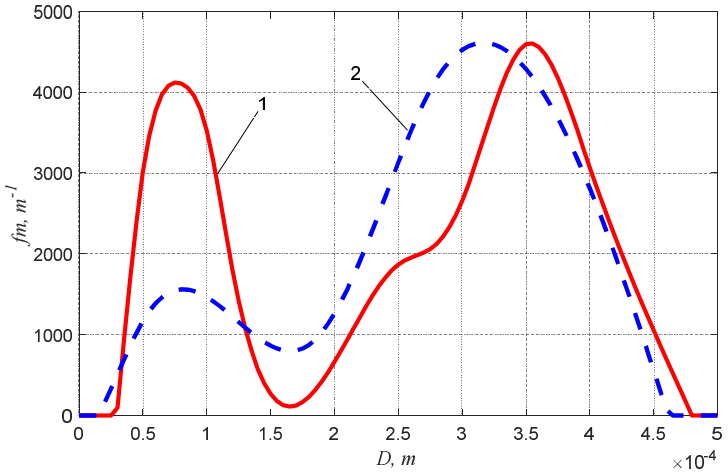


Figure 4: Mass function of size distribution density of agglomerates (1 – burning propellant surface, 2 – nozzle entrance).

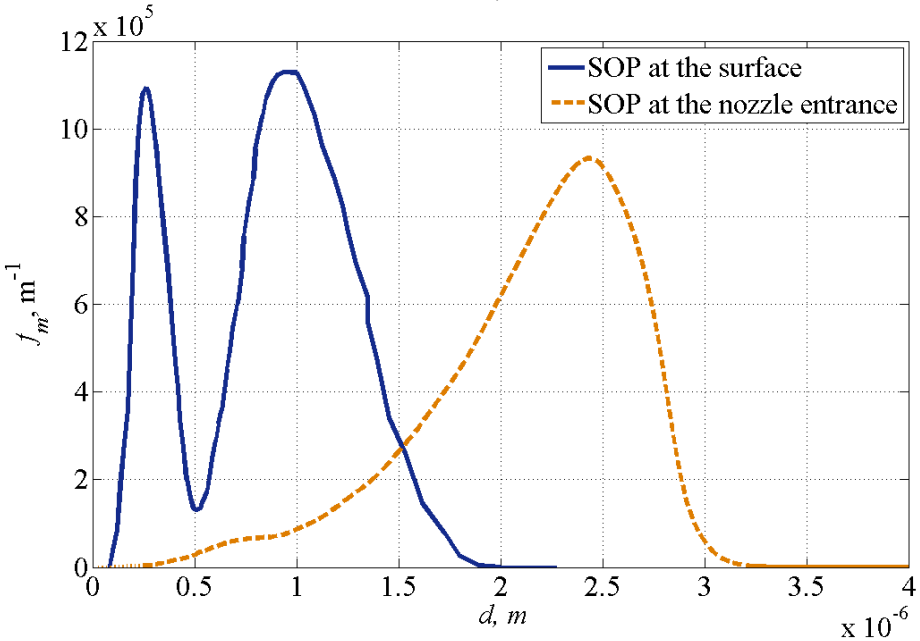


Figure 5: Mass function of size distribution density of smoke oxide particles at surface of the propellant and at the nozzle entrance

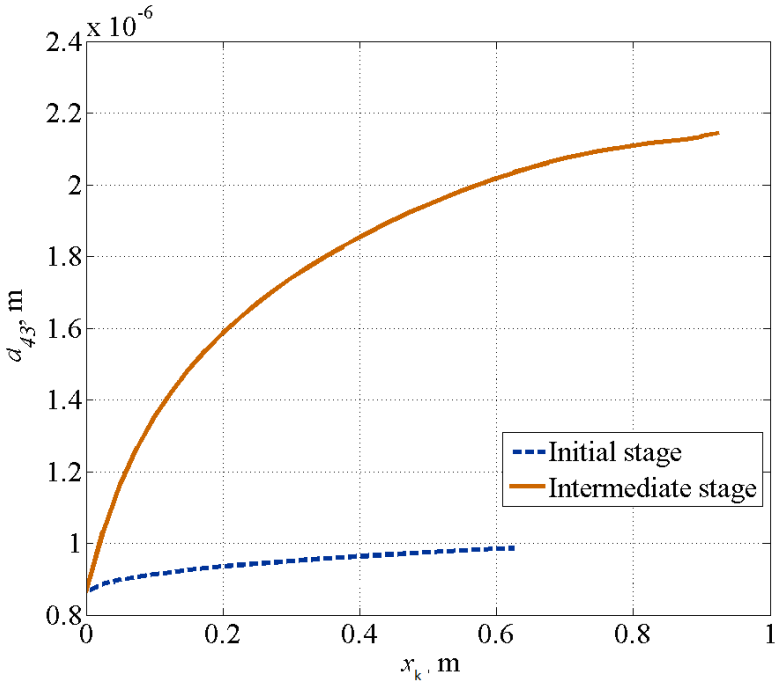


Figure 6: The dependence of the mass average diameter of smoke oxide particles along the curvilinear coordinate

Thus, there is a reason to considers that the influence of CCP evolution in the combustion chamber on the two-phase losses is significant. The estimations [22] indicate that calculated growth of oxide particle can lead to 1.5-2% increase of two-phase losses.

The results of the analysis give reason to talk about a significant influence on motor performance of the evolution of CCP in the combustion chamber. The evolution determines intensity of slag-formation and two-phase losses. Naturally, the intensity of the evolution is different for each motor. It depends on propellant and motor properties. There is no doubt that evolution simulation is important for motor operation modeling.

## Conclusion

In the framework of the present work, a mathematical model of the evolution of a combustion products multiphase flow has been developed for motor conditions. The model is based on the results of an experimental study of formation and evolution of CCP. The effect of the process on the motor performance was analyzed. A significant influence of the process on the slag-formation and two-phase losses of the specific impulse is shown. The utility of the developed models for propulsion studies is shown.

## References

[1] Babuk, V.A., Vasilyev, V.A., and Sviridov, V.V. 2000. Formation of Condensed Combustion Products at the Burning Surface of Solid Rocket Propellant. *Solid Propellant Chemistry, Combustion and Motor Interior Ballistics* / V. Yang, T. B. Brill, W. Z. Ren (Eds). (Progress in Astronautics and Aeronautics, Vol. 185). AIAA, Reston, VA, pp. - 749-776.

[2] Babuk V. A. 2007. Problems in Studying Formation of Smoke Oxide Particles in Combustion of Aluminized Solid Propellants. *Combustion, Explosion, and Shock Waves*. 43(1): 38-45.

[3] Valery A. Babuk. 2017. Formulation Factors and Properties of Condensed Combustion Products. In "Chemical Rocket Propulsion. A Comprehensive Survey of Energetic Materials", pp. 319-341, Springer.

[4] Jackson T. L., Najjar F., Buckmaster J. 2005. New Aluminum Agglomeration Models and Their Use in Solid-Propellant-Rocket Simulations. *Journal of Propulsion and Power*. 21(5): 925-936.

[5] A. Attili, B. Favini, M. Di Giacinto, F. Seraglia. 2009. Numerical Simulation Of Multiphase Flows In Solid Rocket Motors, *45th AIAA/ASME/SAE/ASEE Joint Propulsion Conference & Exhibit*, Denver, Colorado.

[6] Dupays, J., Fabignon, Y., Villedieu, P., Lavergne, G., and Estivalezes, J. L. 2000. Some Aspects of Two-Phase Flows in Solid-Propellant Rocket Motors. *Solid Propellant Chemistry, Combustion and Motor*

*Interior Ballistics* / V. Yang, T. B. Brill, W. Z. Ren (Eds). (Progress in Astronautics and Aeronautics, Vol. 185). AIAA, Reston, VA, pp. — 859–883.

[7] Babuk, V.A., Vasilyev, V.A., and Naslednikov, P.A. 2001. Experimental Study of Evolution of Condensed Combustion Products in Gas Phase of Burning Solid Rocket Propellant. In: *Combustion of Energetic Materials*, edited by K. Kuo and L. De Luca, N.Y., 412-426.

[8] Babuk V.A., Budnyi N.L. 2017. Evolution process of fine fraction of condensed combustion products of aluminized condensed systems: experimental study // MATEC Web of Conferences, 110, 01006.

[9] Babuk V.A., Nizyaev A.A. 2017. Modeling of agglomerates formation and evolution at combustion of aluminized propellants in intra-chamber environments // MATEC Web of Conferences, 110, 01061.

[10] V.A. Babuk, N.L. Budnyi, A.A. Nizyaev. 2019. Mathematical modeling of agglomerates evolution. *EUCASS Book Series Advances in Aerospace Sciences Vol. 11 – Progress in Propulsion Physics,* EUCASS, Torus Press, EDP Sciences. pp. 131-148.

[11] Babuk, V. A., Vasilyev, V. A. 2002. Model of Aluminum Agglomerate Evolution in Combustion Products of Solid Rocket Propellant. *Journal of Propulsion and Power*. 18: 814-824.

[12] Babuk, V. A., Budnyi, N.L. Modeling the formation of oxide during the burning of metal agglomerates. 2015. Chimicheskay phisika i mezoskopiya. 17(1): 39-50. (in Russian)

[13] Babuk, V. A., Budnyi, N.L. 2017. Modeling of the evolution of highly dispersed oxide in the composition of the combustion products flow of aluminized solid propellant. Chimicheskay phisika i mezoskopiya. 19(1): 5-19. (in Russian)

[14] Sternin l. E., Shraiber A. A. 1994. Multiphase flows of gas with particles. Moscow, Mashinostroenie (in Russian).

[15] Reist, P. C. Introduction to Aerosol Science / New York, Macmillan. 1984.

[16] Fuchs, N. A. The mechanics of aerosols / London, Pergamon Press. 1964.

[17] Levich, V. G. Physicochemical Hydrodynamics / Englewood Cliffs, NJ: Prentice-Hall. 1962.

[18] Pearson, H., Valioulis, I., & List, E. 1984. Monte Carlo simulation of coagulation in discrete particle-size distributions. Part 1. Brownian motion and fluid shearing. Journal of Fluid Mechanics. 143: 367-385.

[19] Valery A. Babuk and Alexander A. Nizyaev. 2017. Modeling of Evolution of the Coarse Fraction of Condensed Combustion Products on a Surface of Burning Aluminized Propellant and within a Combustion Products Flow. *International Journal for Energetic Materials and Chemical Propulsions*. 16(1): 22-38.

[20] Babuk, V.A., Vasilyev, V.A., and Malakhov, M.S. 1999. Condensed Combustion Products at the Burning Surface of Aluminized Solid Propellant. *Journal of Propulsion and Power*. 15(6): 783-793.

[21] Orbital ATK Propulsion Product Catalog, 2016, pp. 27.

[22] Glushko V.P. et al. Thermodynamic and thermophysical properties of combustion products. 1971. V. 1. Moscow. VINITI (in Russian).